

Ordering in the Quasi-Two-Dimensional XY Model: the Role of a Small Interplane Coupling

D. Baeriswyl, X. Bagnoud, A. Chiolero and M. Zamora

Institut de Physique Théorique, Université de Fribourg

Pérolles, CH-1700 Fribourg, Switzerland

Received July 8, 1992

The three-dimensional classical XY model is studied for strong coupling J_{\parallel} within planes and weak coupling J_{\perp} between planes. It is found that the interplay between spin waves and vortex loops plays an important role, in particular for $J_{\perp} \ll J_{\parallel}$. The critical temperature is calculated both for a finite number of planes and for the infinite system using various methods, including scaling arguments, mean-field theory, the renormalized harmonic approximation and Monte Carlo simulations. While for a finite number of planes there is no spontaneous magnetization, the infinite system becomes ferromagnetic at low temperatures, as soon as J_{\perp} is finite. As to the two-dimensional XY model, a simple renormalization of the logarithmic interaction between vortices due to the temperature dependence of the spin wave spectrum yields a critical temperature $k_B T_c = 0.96J$, in excellent agreement with Monte Carlo calculations and high-temperature expansions. At the same time the renormalized harmonic approximation for the spin wave excitations provides critical exponents $\eta(T)\delta(T)$, which agree very well with values deduced from a finite size scaling analysis.

I. Introduction

A great variety of critical phenomena, from certain magnetic phase transitions over superfluidity and superconductivity up to ordering in liquid crystals or the roughening transition has been associated with the universality class of the XY model. This model, a collection of interacting two-component spins, is known for its peculiar properties in two spatial dimensions. There is no spontaneous magnetization for all finite temperatures^{1,2}, but nevertheless there exists a phase transition of a special kind. Below a critical temperature and for zero magnetic field the spin-spin correlation function decays algebraically and the magnetic susceptibility is infinite. Thus there exists a critical line with temperature dependent exponents. The transition from this low-temperature phase with algebraic correlations to a high-temperature phase with exponential decay of the correlation functions has been associated with the unbinding of vortex-antivortex pairs (Berezinskii-Kosterlitz-Thouless transition)^{3,4}.

The discovery of high-temperature superconductivity in layered materials has stimulated a renewed interest in the two-dimensional XY model. Despite their layered structure these superconductors are not strictly two-dimensional, as there is always some coupling between adjacent planes, e.g. a Josephson coupling due to tunneling of Cooper pairs. This raises the question to what extent such a coupling, as small as it may be, removes the peculiarities of the Berezinskii-Kosterlitz-

Thouless transition. The aim of this paper is to study this question for an XY model on a simple cubic lattice with strong couplings between nearest neighbor spins for bonds in x- and y-directions and weak couplings in z-direction. It will be shown that the critical temperature T_c for a small but finite coupling in z-direction is slightly larger than the critical temperature T_{KT} of the Berezinskii-Kosterlitz-Thouless transition for uncoupled planes. There is a large region below T_c where the system behaves like the three-dimensional XY model, but at still lower temperatures there is a crossover to a new behavior dominated by vortex loops between the weakly coupled planes.

The paper is organized as follows. Section II presents the two types of excitations, spin waves on the one hand, point vortices (for 2d) and vortex loops (for 3d) on the other hand. The two-dimensional XY model is studied in Section III, with main emphasis on the effects of the renormalization of the spin wave spectrum, both on the critical temperature and on the exponents $\eta(T)$ and $\delta(T)$ along the critical line below T_{KT} . A mean-field approach with respect to the weak coupling in z-direction is used both for the critical temperature (Section IV) and the spontaneous magnetization (Section V). Estimates for T_c on the basis of scaling arguments in the continuum limit (Section IV) are shown to break down for very small interplane couplings. This is attributed to the abundance of vortex loops between the planes (Section VI). A combined study for a finite number of planes, using both analytical approximations

and Monte Carlo simulations, is presented in Section VII. The paper concludes with a brief summary of the results in Section VIII and a few comments on their possible relevance for experiments on layered superconductors.

II. Spin waves, vortices and vortex loops

We consider a simple cubic lattice described by lattice vectors \mathbf{R} and with a lattice constant 1. Our model Hamiltonian is defined as

$$H = - \sum_{\langle \mathbf{R}, \mathbf{R}' \rangle} J(\mathbf{R}, \mathbf{R}') \mathbf{S}(\mathbf{R}) \cdot \mathbf{S}(\mathbf{R}'), \quad (2.1)$$

where $\mathbf{S}(\mathbf{R})$ is a unit vector (a "spin") attached to the site \mathbf{R} and the exchange constants are

$$J(\mathbf{R}, \mathbf{R}') = \begin{cases} J_{\parallel} & \text{for neighbors in the x-y planes,} \\ J_{\perp} & \text{for neighbors in z-direction.} \end{cases} \quad (2.2)$$

The summation in Eq. (2.1) runs over all nearest neighbor pairs. Depending on the context, the spins represent magnetic moments or a phase variable of a complex order parameter. It is often convenient to use the representation in terms of angles $\vartheta(\mathbf{R})$, $-\pi < \vartheta(\mathbf{R}) \leq \pi$,

$$H = - \sum_{\langle \mathbf{R}, \mathbf{R}' \rangle} J(\mathbf{R}, \mathbf{R}') \cos \{ \vartheta(\mathbf{R}) - \vartheta(\mathbf{R}') \}. \quad (2.3)$$

For very low temperatures the directions of neighboring spins deviate very little from each other and, neglecting vortex excitations, we approximate Eq. (2.3) by

$$H \approx -N(2J_{\parallel} + J_{\perp}) + \frac{1}{2} \sum_{\langle \mathbf{R}, \mathbf{R}' \rangle} J(\mathbf{R}, \mathbf{R}') [\vartheta(\mathbf{R}) - \vartheta(\mathbf{R}')]^2, \quad (2.4)$$

where N is the number of sites. Assuming periodic boundary conditions we can diagonalize the Hamiltonian by Fourier transformation

$$\vartheta(\mathbf{R}) = \frac{1}{\sqrt{N}} \sum_{\mathbf{q}} e^{i\mathbf{q} \cdot \mathbf{R}} \vartheta(\mathbf{q}), \quad (2.5)$$

where the wavevectors $q_{\alpha} = 2\pi n_{\alpha}/N_{\alpha}$, $\alpha = x, y, z$ are restricted to the first Brillouin zone, $-\pi < q_{\alpha} \leq \pi$. This yields the Hamiltonian in the spin wave approximation

$$H_s = \frac{1}{2} \sum_{\mathbf{q}} \omega(\mathbf{q}) |\vartheta(\mathbf{q})|^2, \quad (2.6)$$

where

$$\omega(\mathbf{q}) = 4J_{\parallel} \left(\sin^2 \frac{q_x}{2} + \sin^2 \frac{q_y}{2} \right) + 4J_{\perp} \sin^2 \frac{q_z}{2} \quad (2.7)$$

is the spin wave spectrum. It is straightforward to calculate correlation functions using this approximation. According to the "Gaussian averaging theorem" the following relations hold for averages with the Hamiltonian (2.6),

$$\begin{aligned} \langle e^{i\vartheta(\mathbf{R})} \rangle &= e^{-\frac{1}{2}\langle \vartheta^2(\mathbf{R}) \rangle}, & (2.8) \\ \langle e^{i[\vartheta(\mathbf{R}) - \vartheta(\mathbf{R}')] } \rangle &= e^{-\frac{1}{2}\langle [\vartheta(\mathbf{R}) - \vartheta(\mathbf{R}')]^2 \rangle}. & (2.9) \end{aligned}$$

The exponents are easily calculated using Eq. (2.5) together with the relation

$$\langle |\vartheta(\mathbf{q})|^2 \rangle = \frac{k_B T}{\omega(\mathbf{q})}. \quad (2.10)$$

The spin wave spectrum appears not only as a low temperature approximation for the Hamiltonian but also in the Mermin-Wagner theorem. We apply a magnetic field h parallel to the x axis and try to evaluate the magnetization

$$M(h) = \langle S_x(\mathbf{R}) \rangle, \quad (2.11)$$

where the average is taken with respect to the Hamiltonian (2.1) including the magnetic field term

$$H' = -h \sum_{\mathbf{R}} S_x(\mathbf{R}). \quad (2.12)$$

The original approach of Mermin and Wagner¹ or its classical counterpart⁵, derived for an isotropic system, is easily generalized to the present case with two different coupling constants. We obtain the inequality

$$M^2(h) \frac{1}{N} \sum_{\mathbf{q}} \frac{k_B T}{\omega(\mathbf{q}) + hM(h)} \leq 1. \quad (2.13)$$

In order to see whether there is a spontaneous magnetization we have to take first the thermodynamic limit $N \rightarrow \infty$ and then the limit $h \rightarrow 0$, giving

$$M^2 \int \frac{d^3 q}{(2\pi)^3} \frac{k_B T}{\omega(\mathbf{q})} \leq 1. \quad (2.14)$$

In two dimensions (or for $J_{\perp} = 0$ in Eq. (2.7)) the integral diverges because of the long wavelength spin excitations, and therefore there is no spontaneous magnetization at finite temperatures. On the other hand, an arbitrarily small interplane coupling J_{\perp} is sufficient to render the integral finite and to allow for a finite magnetization. This will be discussed in more detail in Section V.

We turn now to the topological excitations which are point vortices in two dimensions and vortex loops

in three dimensions. A systematic way for introducing consistently variables that can be associated with vortices in two and vortex loops in three dimensions, respectively, has been devised by Savit⁶ (see also Ref. 7). In two dimensions the low temperature limit of the partition function is

$$Z = Z_s \cdot \sum_{\{m(\mathbf{R})\}} \exp \left\{ \pi\beta J \sum_{\mathbf{R} \neq \mathbf{R}'} m(\mathbf{R}) \log |\mathbf{R} - \mathbf{R}'| m(\mathbf{R}') \right\} \cdot \exp \left\{ -\pi\beta J c \sum_{\mathbf{R}} m^2(\mathbf{R}) \right\}, \quad (2.15)$$

where Z_s is the partition function in spin wave approximation and the constant c is given by

$$c = \gamma + \frac{3}{2} \log 2, \quad (2.16)$$

γ being the Euler constant. The summation in Eq. (2.15) is restricted to (finite energy) configurations satisfying the constraint

$$\sum_{\mathbf{R}} m(\mathbf{R}) = 0. \quad (2.17)$$

We notice that in the low temperature limit ($\beta J \gg 1$) the partition function is factorized into two independent contributions, a spin wave part and a term corresponding to an overall neutral 2d Coulomb gas. The integer variables $m(\mathbf{R})$ can be interpreted as point vortices. This correspondence between (topological) charges and spin vortices appears explicitly in the framework of the Villain model^{8,9}. The generalization of Savit's derivation for the 3d Hamiltonian (2.3) is given in Appendix A. The partition function can be written as

$$Z = Z_s \cdot \sum_{\{\ell_\mu(\mathbf{R})\}} \exp \left\{ -2\pi^2 \beta \sum_{\mathbf{R}, \mathbf{R}', \mu} \ell_\mu(\mathbf{R}) V_\mu(\mathbf{R} - \mathbf{R}') \ell_\mu(\mathbf{R}') \right\}, \quad (2.18)$$

where the vectors \mathbf{R} denote the sites of the dual lattice, $\ell_\mu(\mathbf{R})$, and $\mu = x, y, z$, are integers satisfying the constraint

$$\sum_{\mu} [\ell_\mu(\mathbf{R}) - \ell_\mu(\mathbf{R} - \mathbf{e}_\mu)] = 0, \quad (2.19)$$

\mathbf{e}_μ being a unit vector in direction μ . The interaction is given by

$$V_\mu(\mathbf{R} - \mathbf{R}') = \begin{cases} J_\perp V(\mathbf{R} - \mathbf{R}') & , \quad \mu = x, y, \\ J_\parallel V(\mathbf{R} - \mathbf{R}') & , \quad \mu = z, \end{cases} \quad (2.20)$$

where

$$V(\mathbf{R} - \mathbf{R}') = \frac{1}{N} \sum_{\mathbf{q}} \frac{e^{i\mathbf{q}(\mathbf{R} - \mathbf{R}')}}{\omega(\mathbf{q})/J_\parallel}. \quad (2.21)$$

In analogy to the point vortices of the 2d model one can also introduce topological excitations for the 3d model. These are associated with the integer valued variables $\ell_\mu(\mathbf{R})$ and are called vortex lines. An example of a vortex loop parallel to the $x - y$ plane is illustrated in Figure 1.

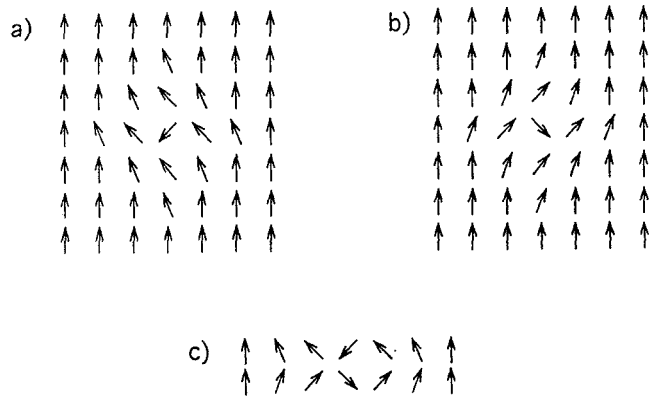


Figure 1: Spin configuration for an elementary vortex loop between the XY planes: a) upper x-y plane, b) lower x-y plane, c) cut along the x-z plane.

III. The Berezinskii - Kosterlitz - Thouless transition

In this Section we summarize the critical behavior of the two-dimensional XY model ($J_\parallel = J, J_\perp = 0$ in Eq. (2.2)), as some of its properties will be used later on. We consider first the low temperature regime. In spin wave approximation the spin-spin correlation function is obtained using Eqs. (2.9) and (2.10). For large distances $|\mathbf{R} - \mathbf{R}'|$ one finds (see [5] for a detailed derivation)

$$\frac{1}{2} \langle [\vartheta(\mathbf{R}) - \vartheta(\mathbf{R}')]^2 \rangle \sim \frac{k_B T}{2\pi J} [\log(|\mathbf{R} - \mathbf{R}'|) + c], \quad (3.1)$$

where c is given by Eq. (2.16). This yields a power law decay

$$\langle \cos [\vartheta(\mathbf{R}) - \vartheta(\mathbf{R}')] \rangle \sim |\mathbf{R} - \mathbf{R}'|^{-\eta} \quad (3.2)$$

with an exponent

$$\eta = \frac{k_B T}{2\pi \tilde{J}}. \quad (3.3)$$

The magnetization $M(\mathbf{h})$ due to a magnetic field term (2.12) is calculated in a similar way. In spin wave approximation the Hamiltonian is again given by Eq. (2.6) with $\omega(\mathbf{q})$ replaced by

$$\omega(\mathbf{q}) = 4J \left(\sin^2 \frac{q_x}{2} + \sin^2 \frac{q_y}{2} \right) + \frac{1}{2}h. \quad (3.4)$$

Replacing the trigonometric functions by their long-wavelength limits and integrating over a circular domain of radius $q_0 = 2\sqrt{\pi}$ (instead of the Brillouin zone) we find

$$\frac{1}{2} \langle \vartheta^2(\mathbf{R}) \rangle \approx \frac{k_B T}{8\pi J} \log \frac{Jq_0^2 + h}{h}. \quad (3.5)$$

Together with Eq. (2.8) this yields the magnetization for $h \rightarrow 0$

$$M(h) = \langle S_x(\mathbf{R}) \rangle \approx \left(\frac{h}{Jq_0^2} \right)^{1/\delta}. \quad (3.6)$$

with a critical exponent

$$\delta = \frac{8\pi J}{k_B T}. \quad (3.7)$$

The equations (3.2) and (3.6) are the same as those found at a critical point in ordinary second order phase transitions. However here the critical behavior extends over a whole line of critical points with temperature dependent exponents. We notice that the scaling law

$$d \frac{\delta - 1}{\delta + 1} = 2 - \eta, \quad (3.8)$$

is fulfilled to leading order in T .

How to proceed to take into account the nonlinearities of the interaction? A simple method that has been used frequently in the theory of structural phase transitions¹⁰ is the renormalized harmonic approximation where one introduces an effective harmonic Hamiltonian H_0 of the form (2.4) with \mathbf{J} replaced by a temperature dependent variational parameter $\tilde{\mathbf{J}}$. The Bogoliubov inequality for the free energy

$$G \leq G_0 + \langle H - H_0 \rangle_0, \quad (3.9)$$

where both G_0 and the average are evaluated with respect to H_0 , yields a variational principle. Thus $\tilde{\mathbf{J}}$ is determined by minimizing the r.h.s. of Eq. (3.9). In the present context this program can be explicitly carried out and one finds¹¹

$$\frac{\tilde{J}}{J} = \exp \left(-\frac{k_B T}{4\tilde{J}} \right) \quad (3.10)$$

\tilde{J} is always smaller than \mathbf{J} and allows for larger fluctuations than the simple spin wave approximation (2.6). A solution of (3.10) exists only for $T < T_c = (4/e)J/k_B$. In this approximation both the power law decay of the spin correlations (3.2) and the critical dependence of the magnetization on the magnetic field (3.6) are unchanged, except that in the expressions for the critical exponents, Eqs. (3.3) and (3.6), \mathbf{J} has to be replaced by \tilde{J} .

A radically different picture has been devised by Kosterlitz and Thouless⁴. One can understand it starting from the factorized partition function (2.15), where a phase transition can only come from the vortex excitations coupled by a logarithmic interaction potential. At low temperatures the energy term dominates over the entropy term in the free energy and the vortex-antivortex pairs are confined. The power law decay of the spin correlations due to the spin waves is practically unaffected by the topological excitations. Thus the magnetic susceptibility is infinite, while, in view of the Mermin-Wagner theorem, the magnetization vanishes. At high temperatures the entropy term dominates and the vortices become free; it follows that the spin correlations decay exponentially and the susceptibility is finite.

A detailed analysis of the region close to the critical temperature has been carried out by Kosterlitz¹² using a renormalization group technique. He obtained a fixed point solution, which he attributed to the critical point where the unbinding of vortex-antivortex pairs sets in. The critical temperature T_{KT} is given by the solution of the equation

$$\frac{\pi J}{2k_B T_{KT}} - 1 = 2\pi \exp \left\{ -\frac{\pi^2 J}{2k_B T_{KT}} \right\}, \quad (3.11)$$

with the numerical value $k_B T_{KT} = 1.35J$. In approaching T_{KT} from above, the renormalization group analysis yields both a diverging correlation length

$$\xi \sim \exp \left\{ b \left(\frac{T_{KT}}{T - T_{KT}} \right)^\sigma \right\}, \quad (3.12)$$

and a diverging susceptibility

$$\chi \sim \xi^{2-\eta}, \quad (3.13)$$

where $b \approx 1.5$, $\eta = \frac{1}{4}$, and $\sigma = \frac{1}{2}$.

Recently this rather peculiar phase transition has been reanalyzed both using an elaborate high-temperature expansion¹³ and finite-size scaling combined with the theory of conformal invariance¹⁴. Both approaches are consistent with Eqs. (3.12) and (3.13) with constants $k_B T_{KT} = 0.90J$, $b = 1.58$, $\eta = 0.25$, $a =$

$\frac{1}{2}$ [13] and $k_B T_{KT} \propto J, \eta \approx 0.23, \sigma = 0.50$ [14], respectively. We notice that these values agree very well with the results of the renormalization group analysis by Kosterlitz except for the value of the critical temperature, where there is a discrepancy of about 50%. The rather serious disagreement in the values of T_{KT} is somewhat puzzling, since renormalization group methods have been very successful in predicting T_c for the case of the two-dimensional Ising model¹⁵. We attribute it to anharmonicity effects on the spin wave excitations which have been neglected in Eq. (2.15). As pointed out above, these effects can approximately be taken into account by replacing the coupling constant J by a renormalized coupling $\tilde{J}(T)$. This leads to a reduction of both the chemical potential and the interaction energy for vortex excitations. The critical temperature is then calculated by replacing J by $\tilde{J}(T)$ in Eq. (3.11), where $\tilde{J}(T)$ is given by Eq. (3.10). Thus T_{KT} is obtained as solution of the equation

$$k_B T = 1.35 \tilde{J}(T). \quad (3.14)$$

We find $k_B T_{KT} = 0.96J$, which is very close to the values deduced from high-temperature series and finite size scaling. Further support for our analysis comes from a comparison between the critical exponents η obtained on the basis of the renormalized harmonic approximation and those extracted from the finite size scaling. This is illustrated in Figure 2. We conclude that the temperature dependence of the power law decay of spin correlations below T_{KT} is dominated by the renormalization of the spin wave spectrum due to anharmonicity.

IV. Critical temperature

We return now to the 3d XY model with (strong) coupling J_{\parallel} in x - and y - directions and (weak) coupling J_{\perp} along the z axis. For very small couplings J_{\perp} , we expect to be in some sense close to the 2d limit, so that a mean-field approximation with respect to J_{\perp} appears to be reasonable. In this Section we discuss the magnetic susceptibility for $T > T_c$; the order parameter for $T < T_c$ will be treated in Section V.

A brief derivation for the 3d susceptibility in mean-field approximation with respect to J_{\perp} is given in Appendix B. The result is

$$\chi_{3d} = \frac{\chi_{2d}}{1 - 2J_{\perp}\chi_{2d}}, \quad (4.1)$$

where χ_{2d} is the susceptibility for $J_{\perp} = 0$, i.e. for the 2d case. The divergence of χ_{3d} defines the critical temperature T_c through the relation

$$2J_{\perp}\chi_{2d}(T_c) = 1. \quad (4.2)$$

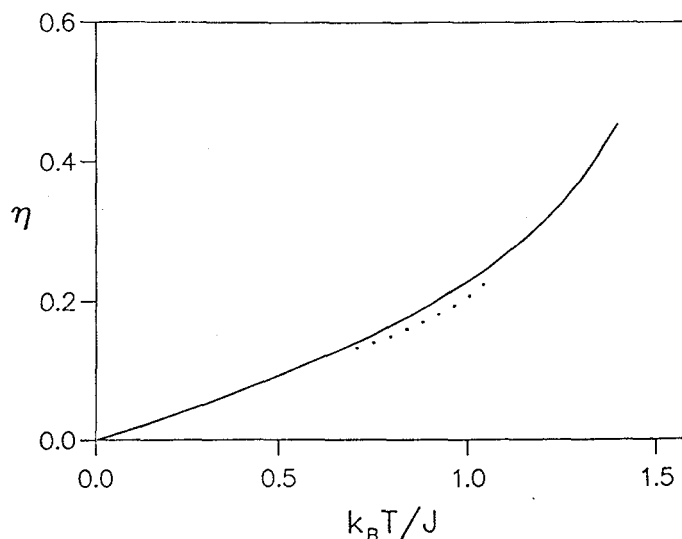


Figure 2: Critical exponent $\eta(T)$ in the renormalized harmonic approximation (full line) and from finite size scaling (dotted line).

For very small J_{\perp} χ_{2D} has to be very large, so that we can use the asymptotic behavior (3.13),

$$\chi \sim \chi_0 \exp \left\{ (2 - \eta)b \left(\frac{T_{KT}}{T - T_{KT}} \right)^{\frac{1}{2}} \right\}, \quad (4.3)$$

where χ_0 is an unknown constant. Inserting this expression into Eq. (4.2) we find

$$T_c = T_{KT} \left\{ 1 + \left[\frac{(2 - \eta)b}{\log(2J_{\perp}\chi_0)} \right]^2 \right\}, \quad (4.4)$$

in qualitative agreement with an earlier study using a different argument¹⁶. Therefore T_c increases as a function of J_{\perp} , starting with an infinite slope at T_{KT} for $J_{\perp} = 0$. For general couplings J_{\perp} we use the high-temperature expansion for χ_{2D} of Butera et al.¹³. The result for T_c is shown in Figure 3 in comparison with a recent Monte Carlo simulation¹⁷. The mean-field result agrees qualitatively with the simulation, although the mean-field temperatures are consistently higher than the Monte Carlo data. The quantitative discrepancy is undoubtedly due to the neglect of interplane fluctuations.

It is illuminating to use scaling in order to map the anisotropic case ($J_{\parallel} \neq J_{\perp}$) onto an isotropic model. The only requirement is the validity of the continuum limit of Eq. (2.1),

$$H = \frac{1}{2} \int d^3x \left\{ J_{\parallel} [\nabla_{\parallel} \mathbf{S}(\mathbf{x})]^2 + J_{\perp} [\partial_z \mathbf{S}(\mathbf{x})]^2 \right\}. \quad (4.5)$$

The transformation

$$(x, y, z) = \left(\sqrt{\gamma}x', \sqrt{\gamma}y', \frac{z'}{\gamma} \right) \quad (4.6)$$

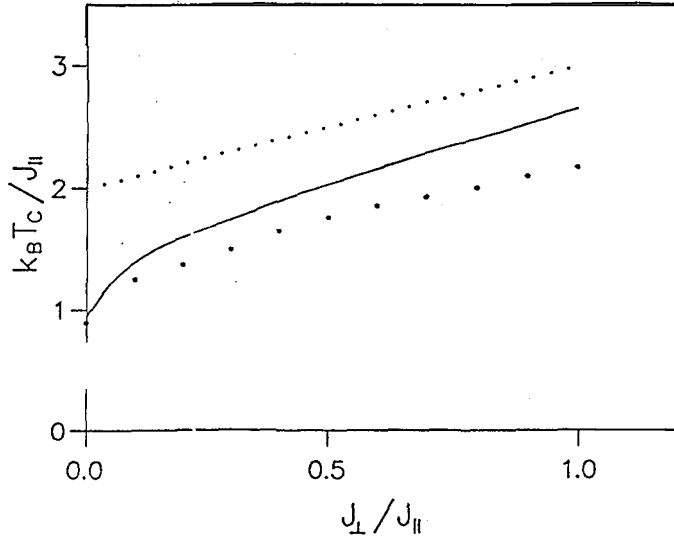


Figure 3: Critical temperature as a function of the anisotropy in mean-field approximation with respect to J_{\perp} (full line) from Monte Carlo simulations (dots) and in mean-field approximation with respect to all couplings (dotted line).

(with Jacobian = 1), where

$$\gamma = (J_{\parallel}/J_{\perp})^{1/3}, \quad (4.7)$$

yields indeed an isotropic 3d model

$$H = \frac{1}{2} J_{\parallel}^{\frac{2}{3}} J_{\perp}^{\frac{1}{3}} \int d^3x [\nabla \mathbf{S}(\mathbf{x})]^2. \quad (4.8)$$

Together with the known value of the critical temperature of the isotropic 3d XY model^{17,18} (with exchange constant J), $k_B T_c \approx 2.2J$ we find (for fixed J_{\parallel})

$$T_c \sim (J_{\perp}/J_{\parallel})^{\frac{1}{3}}. \quad (4.9)$$

This behavior is compared to the Monte Carlo results in Figure 4. We notice that there is excellent agreement between the two sets of data for $J_{\perp}/J_{\parallel} \geq 0.2$. The deviations for $J_{\perp}/J_{\parallel} \leq 0.2$ can be attributed to the abundance of vortex loops parallel to the $x-y$ planes, invalidating the continuum limit. This will be discussed in Section VI.

It is also worthwhile to use scaling for the associated Ginzburg-Landau free-energy functional

$$\begin{aligned} \beta F = \sum_{\mathbf{R}} \left\{ \frac{1}{8J_0} \sum_{\alpha=1}^2 [J_{\parallel} (\Delta_x \psi_{\alpha}(\mathbf{R}))^2 \right. \\ \left. + J_{\parallel} (\Delta_y \psi_{\alpha}(\mathbf{R}))^2 + J_{\perp} (\Delta_z \psi_{\alpha}(\mathbf{R}))^2] \right. \\ \left. + \frac{1}{4} \left(\frac{1}{\beta J_0} - 1 \right) |\psi(\mathbf{R})|^2 + \frac{1}{64} |\psi(\mathbf{R})|^4 \right\}, \end{aligned} \quad (4.10)$$

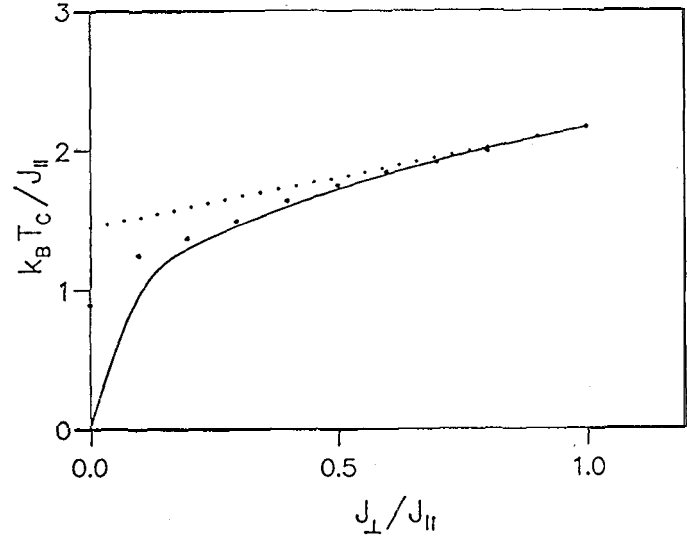


Figure 4: Critical temperature as a function of anisotropy from scaling (full line), Ginzburg-Landau theory (dotted line) and Monte Carlo (dots).

where Δ_{μ} , $\mu = x, y, z$ are lattice derivatives and $J_0 = 2J_{\parallel} + J_{\perp}$. The partition function is given by

$$Z = \prod_{\mathbf{R}, \alpha} \left[\int_{-\infty}^{\infty} \frac{d\psi_{\alpha}(\mathbf{R})}{4\pi\beta J_0} \right] \exp(-\beta F\{\psi_{\alpha}(\mathbf{R})\}), \quad (4.11)$$

where α numbers the two components of the field $\psi = (\psi_1, \psi_2)$. Eq. (4.10) is derived in Appendix C. The free energy functional (4.10) represents an expansion in powers of both ψ and $\Delta_{\mu}\psi$, which limits the applicability of the Ginzburg-Landau theory. In the continuum limit the transformation (4.6) together with the rescaled fields

$$\psi'(x', y', z') = \psi(x, y, z), \quad (4.12)$$

yields the free energy functional

$$\begin{aligned} \beta F = \int d^3x' \left\{ \frac{1}{8\mu} |\nabla' \psi'|^2 \right. \\ \left. + \frac{1}{4} \left(\frac{1}{\beta J_0} - 1 \right) |\psi'|^2 + \frac{1}{64} |\psi'|^4 \right\}, \end{aligned} \quad (4.13)$$

where $\mu = J_0 / (J_{\parallel}^{2/3} J_{\perp}^{1/3})$. An additional scale transformation

$$\mathbf{x}' = \mu \mathbf{x}'', \quad \psi'(\mathbf{x}') = \psi''(\mathbf{x}''), \quad (4.14)$$

yields the isotropic Ginzburg-Landau theory with effective exchange constant J_0 , up to a multiplicative constant in front of the free energy. This constant cannot change the ratio between the exact critical temperature

T_c and the mean-field value J_0/k_B . Therefore for fixed J_{\parallel} the critical temperature scales as

$$T_c \sim J_0/J_{\parallel} = 2 + \frac{J_{\perp}}{J_{\parallel}}. \quad (4.15)$$

Close to the isotropic limit this result agrees with Eq. (4.9). The deviations between the two expressions for small J_{\perp} (see Figure 4) are due to the additional approximations of the Ginzburg-Landau theory, in particular the expansion up to second order in the gradient term $\partial_z \psi$.

V. Order parameter

In Section III we have presented several arguments indicating that for the $2d$ XY model there exists a critical line defined by $h = 0, 0 < T \leq T_{KT}$, where there is no spontaneous magnetization and both the correlation length ξ and the magnetic susceptibility χ are infinite. Therefore an arbitrarily small coupling J_{\perp} will have a dramatic effect on the ordering in the 3d case. This is confirmed by a simple spin wave approximation¹¹. Eqs. (2.8) and (2.10) yield the following expression for the order parameter

$$M = \langle \cos \vartheta(\mathbf{R}) \rangle = \exp \{ -\alpha k_B T / (2J_{\parallel}) \}, \quad (5.1)$$

where

$$\alpha = \int \frac{d^3 q}{(2\pi)^3} \frac{J_{\parallel}}{\omega(\mathbf{q})}, \quad (5.2)$$

and the spin wave spectrum is given by Eq. (2.7). The integration in Eq. (5.2) is performed over the Brillouin zone $-\pi < q_{\alpha} \leq \pi, \alpha = x, y, z$. The integral is dominated by small q values and thus we replace the Brillouin zone by a cylindrical domain of equal volume, i.e. of radius $2\sqrt{\pi}$ and height 2π . The error introduced by this approximation is of the order of a few percent. In the limit of large anisotropy, $J_{\perp} \ll J_{\parallel}$, we obtain

$$\alpha \approx \frac{1}{4\pi} \log(4\pi J_{\parallel}/J_{\perp}). \quad (5.3)$$

For $J_{\perp} \rightarrow 0$, α diverges and the order parameter (5.1) tends to zero. But since this divergence is only logarithmic, an extremely small J_{\perp} is sufficient to stabilize a magnetization per site of order 1. This same extreme sensitivity with respect to interplane coupling appears in the Mermin-Wagner upper bound for the magnetization. The application of Eq. (2.14) to the present case yields the inequality

$$M \leq \left(\frac{J_{\perp}}{k_B T a} \right)^{1/2}, \quad (5.4)$$

For $J_{\perp} > 0.01 J_{\parallel}$ the r.h.s. is already larger than the simple mean-field order parameter (with respect to both J_{\parallel} and J_{\perp}), which renders the inequality useless.

The spin wave approximation is valid only at very low temperatures. In order to describe the whole region below the critical temperature, we use the mean-field approach introduced in the previous section. For $J_{\perp} = 0$ and $T < T_{KT}$ the magnetization in an external field h behaves as

$$M(h, T) \sim \left[\frac{h}{h_0(T)} \right]^{1/\delta(T)}, \quad h \rightarrow 0. \quad (5.5)$$

The critical exponent $\delta(T)$ and the function $h_0(T)$ will be discussed later on. For $J_{\perp} \neq 0$ and $h = 0$, the spontaneous magnetization is obtained in mean-field approximation from Eq. (5.5) simply by replacing h by $2J_{\perp} M$, giving

$$M(0, T) = \left[\frac{2J_{\perp}}{h_0(T)} \right]^{1/[\delta(T)-1]}. \quad (5.6)$$

The region $T_{KT} < T < T_c$ requires special considerations. Here the leading term to the magnetization is linear in h ; therefore we replace Eq. (5.6) by

$$M(h, T) = \chi h + \chi_3 h^3 \quad (5.7)$$

(the second order term vanishes by symmetry). Proceeding as above we obtain the spontaneous magnetization for $J_{\perp} \neq 0, h = 0$ in the temperature domain $T_{KT} < T < T_c$,

$$M^2(0, T) = \frac{1 - 2J_{\perp}\chi}{(2J_{\perp})^3 \chi_3}. \quad (5.8)$$

The critical temperature is again given by Eq. (4.2). Unfortunately the expansion (5.7) is not applicable very close to T_{KT} , as all the nonlinear susceptibilities $\chi_{2\ell+1}$ are expected to diverge. For a quantitative determination of the order parameter we therefore limit ourselves to the region below T_{KT} .

We have seen in Section III that the critical exponent η derived within the renormalized harmonic approximation is in good agreement with the values found on the basis of finite size scaling. Therefore we use the same approximation for the functions $h_0(T)$ and $\delta(T)$ in Eq. (5.6). It is not surprising that for $J_{\perp} = 0, h \neq 0$ we obtain the spin wave result, Eqs. (3.6) and (3.7), with \mathbf{J} replaced by \tilde{J}_{\parallel} . The function $h_0(T)$ in Eq. (5.6) is thus given by

$$h_0(T) = 4\pi \tilde{J}_{\parallel}(T), \quad (5.9)$$

where the effective coupling \tilde{J}_{\parallel} is determined by Eq. (3.10). It is interesting to compare this mean-field result for low temperatures,

$$M_m(0, T) \approx \left(\frac{J_{\perp}}{2\pi \tilde{J}_{\parallel}} \right)^{k_B T / (8\pi \tilde{J}_{\parallel})}, \quad (5.10)$$

with the corresponding spin wave expression, deduced from Eqs. (5.1) and (5.3),

$$M_z(0, T) = \left(\frac{J_\perp}{4\pi J_\parallel} \right)^{k_B T / (8\pi J_\parallel)} \quad (5.11)$$

The two expressions agree up to a factor of 2; this originates from the interplane fluctuations taken into account in the spin wave analysis but not in mean-field theory with respect to J_\perp . The results are shown in Figure 5, where the region above T_{KT} has to be considered as an educated guess.

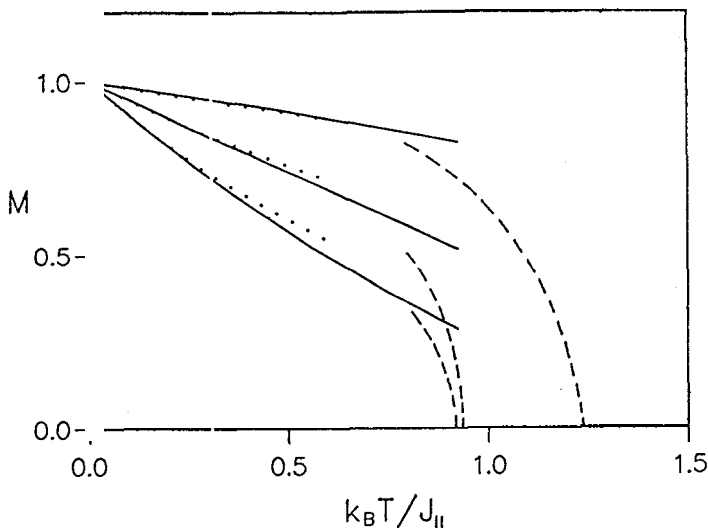


Figure 5: Order parameter in spin wave approximation (dotted lines) and in renormalized harmonic approximation (full lines) for three different anisotropies: $J_\perp/J_\parallel = 10^{-1}, 10^{-5}, 10^{-10}$ (top to bottom). The dashed lines represent our guess for the behavior close to T_c .

VI. The role of parallel vortex loops

We have seen in Section IV that the continuum limit in z -direction breaks down for very small J_\perp and temperatures of the order of T_{KT} . In this Section we argue that this is due to the appearance of parallel vortex loops. The particular role of these topological excitations has been emphasized by Friedel^{19,20} and later studied more thoroughly by Korshunov²¹.

We have shown in Section II (and in more detail in Appendix A) that the partition function for the 3d XY model with coupling constants J_\parallel in x - and y -directions and J_\perp in z -direction can be approximately factorized in the low temperature limit into two independent contributions, the first representing purely harmonic spin wave excitations, the second a gas of interacting vortex loops. Any phase transition has to come from the second factor defined in terms of energies

$$E(\{\ell_\mu(\mathbf{R})\}) = 2\pi^2 \sum_{\mathbf{R}, \mathbf{R}'} V(\mathbf{R} - \mathbf{R}') \cdot \{J_\perp [\ell_x(\mathbf{R})\ell_x(\mathbf{R}') + \ell_y(\mathbf{R})\ell_y(\mathbf{R}')] + J_\parallel \ell_z(\mathbf{R})\ell_z(\mathbf{R}')\}, \quad (6.1)$$

where $V(\mathbf{R} - \mathbf{R}')$ is given by Eq. (2.21) and the integers $\ell_\mu(\mathbf{R})$ have to satisfy the constraint (2.19), i.e. the associated links form closed loops on the (dual) lattice. It is not difficult to calculate the energies (6.1) of elementary loops parallel and perpendicular to the planes, illustrated in Figure 6. In the limit of very small couplings $J_\perp (J_\perp \ll J_\parallel)$ we find

$$E_\parallel = 8\pi^2 J_\perp [V(0) - V(\mathbf{e}_x)] \quad (6.2)$$

for parallel vortex loops and

$$E_\perp = 4\pi^2 J_\parallel [V(0) - V(\mathbf{e}_x)] \quad (6.3)$$

for perpendicular loops. The values of the lattice Green's functions $V(\mathbf{R})$ are easily calculated by integrating over a cylindrical volume of radius $2\sqrt{\pi}$, giving

$$V(0) - V(\mathbf{e}_x) \approx \frac{1}{4\pi} (\log \pi + 2\gamma), \quad (6.4)$$

where $\gamma \approx 0.5772$ is Euler's constant. Eq (6.2) suggests that the energy E_\parallel of an elementary loop parallel to the XY planes is arbitrarily small for $J_\perp \rightarrow 0$, whereas the energy E_\perp of a perpendicular loop is comparable to that of a vortex-antivortex pair in the 2d XY model, $E \approx 2\pi J_\parallel (\frac{3}{2} \log 2 + \gamma)$. While this latter agreement is very satisfactory, the vanishing of E_\parallel for $J_\perp = 0$ is quite puzzling. In fact, a quick look at the configuration of a parallel loop (Figure 1) shows that, besides an energy proportional to J_\perp due to misaligned spins on different planes, there must be a term proportional to J_\parallel due to misalignments within the planes adjacent to the vortex loop. A possible resolution of this paradox is to admit that a given configuration of spins like that of Figure 1 contains both vortex and spin wave degrees of freedom. The contribution of the vortex variables yields a bare energy representing the local effect of the singularity, whereas the spin wave variables describe the relaxation of the lattice surrounding the singularity. In fact, explicit calculations confirm that the elastic energy due to the lattice relaxation yields the dominant contribution to the energy of a parallel vortex loop¹⁹. If this interpretation is correct, the factorization of the partition function into a spin wave part and a vortex part appears as a mere mathematical separation of variables; in a physical vortex excitation both types of variables are necessarily involved.

Apart from these fundamental questions it appears to be rather clear that the excitation of parallel vortex loops requires less energy than that of perpendicular loops. This is visible in Monte Carlo simulations²²,

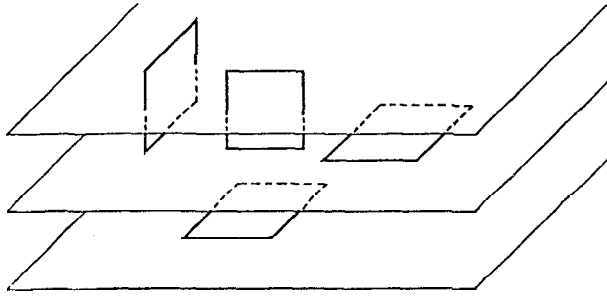


Figure 6: Elementary vortex loops both parallel and perpendicular to the x-y planes.

which show that for $J_{\perp} \ll J_{\parallel}$ the majority of vortex loops is parallel to the x-y planes (for $T \sim T_{KT}$). This has an immediate consequence for the scaling arguments presented in Section IV. A large number of parallel vortex loops corresponds to a configuration where spins on neighboring planes deviate rather strongly from each other, thus invalidating the continuum limit. The discrepancy between the scaling prediction for T_c and the Monte Carlo results for $J_{\perp} \leq 0.1J_{\parallel}$ (Figure 4) undoubtedly originates from this effect. We may then tentatively conclude that in this region of weak couplings J_{\perp} the parallel vortex loops play an essential role. Nevertheless the universality principle implies that there is no change in the critical behavior as a function of J_{\perp}/J_{\parallel} , as long as J_{\perp} is finite.

VII. Finite number of planes

In this Section we consider a finite number of planes stacked along the z axis with a coupling J_{\perp} between planes (and a coupling J_{\parallel} within planes). This problem is not of particular interest for its critical behavior, which is expected to be identical to that of a single plane. In fact, as soon as the correlation length perpendicular to the planes exceeds the thickness of the layer, the system becomes effectively two-dimensional. This is confirmed by the Mermin-Wagner theorem. The spin wave spectrum for M planes consists of M two-dimensional energy bands

$$M^2(\mathbf{q}_{\parallel}, \lambda) = \omega_{\parallel}(\mathbf{q}_{\parallel}) + \omega_{\perp}(\lambda), \lambda = 1, \dots, M, \quad (7.1)$$

where $\omega_{\parallel}(\mathbf{q}_{\parallel})$ is the 2d spin wave spectrum and the lowest of the eigenvalues $\omega_{\perp}(\lambda)$ vanishes due to the continuous symmetry of the Hamiltonian (2.4). For infinitely extended planes and $\hbar \rightarrow 0$ the inequality (2.13) is replaced by

$$M^2(0) \sum_{\lambda=1}^M \int \frac{d^2q}{(2\pi)^2} \frac{k_B T}{\omega_{\parallel}(\mathbf{q}_{\parallel}) + \omega_{\perp}(\lambda)} \leq 1. \quad (7.2)$$

Since one of the eigenvalues $\omega_{\perp}(\lambda)$ vanishes, one of the integrals diverges and there is no spontaneous magnetization whatever the number of planes.

The interest of this system comes from experiments on superfluid films of variable thickness²³ or on thin superconducting layers consisting of a well defined number of planes²⁴⁻²⁸. The relevance of the XY model for these systems will be briefly discussed in the final section. The number of planes M allows to provide additional insight, as various quantities are expected to depend sensitively on M. We limit ourselves to the critical temperature of the phase transition, which should still be of the Kosterlitz-Thouless type. It is straightforward to extend the mean-field analysis of Section 4 to the present case, using open boundary conditions. Some details are given in Appendix B. The critical temperature is given by the solution of the equation

$$2J_{\perp} \cos\left(\frac{\pi}{M+1}\right) \chi_{2d}(T_c) = 1, \quad (7.3)$$

where $\chi_{2d}(T)$ is the magnetic susceptibility for the 2d XY model with exchange constant J_{\parallel} . Eq. (7.3) coincides with Eq. (4.2) in the limit $M \rightarrow \infty$. Figure 7 shows the critical temperature (7.3) as a function of M for different ratios J_{\perp}/J_{\parallel} . We have again used the high temperature series of Butera et al.¹³ for the 2d susceptibility.

In addition to these analytical calculations, where the coupling J_{\perp} is treated in mean-field approximation, we have performed Monte Carlo simulations. The technical details that allowed us to obtain the critical temperature to a high degree of accuracy are explained in Appendix D. The results shown also in Figure 7 confirm the earlier conclusion that the mean-field treatment of the interplane coupling neglects part of the fluctuations and thus yields appreciably higher critical temperatures as compared to Monte Carlo data, except for very small couplings J_{\perp} . Our results, partly published earlier²⁹, are in good agreement with similar computations by Schmidt and Schneider³⁰.

VIII. Discussion

In this paper we have studied the role of dimensionality on ordering and fluctuations for the classical XY model. We have seen that a good understanding of the interplay between small amplitude fluctuations (spin waves) and large amplitude excitations (point vortices and vortex loops) is necessary for describing the phase transition from a paramagnetic high temperature regime to a phase with long-range order in 3d or algebraic order in 2d at low temperatures. For the two-dimensional XY model with its unusual (Kosterlitz-Thouless) transition we have found a very simple way to take into account this interplay. A simple renormalization of the logarithmic interaction between (topologi-

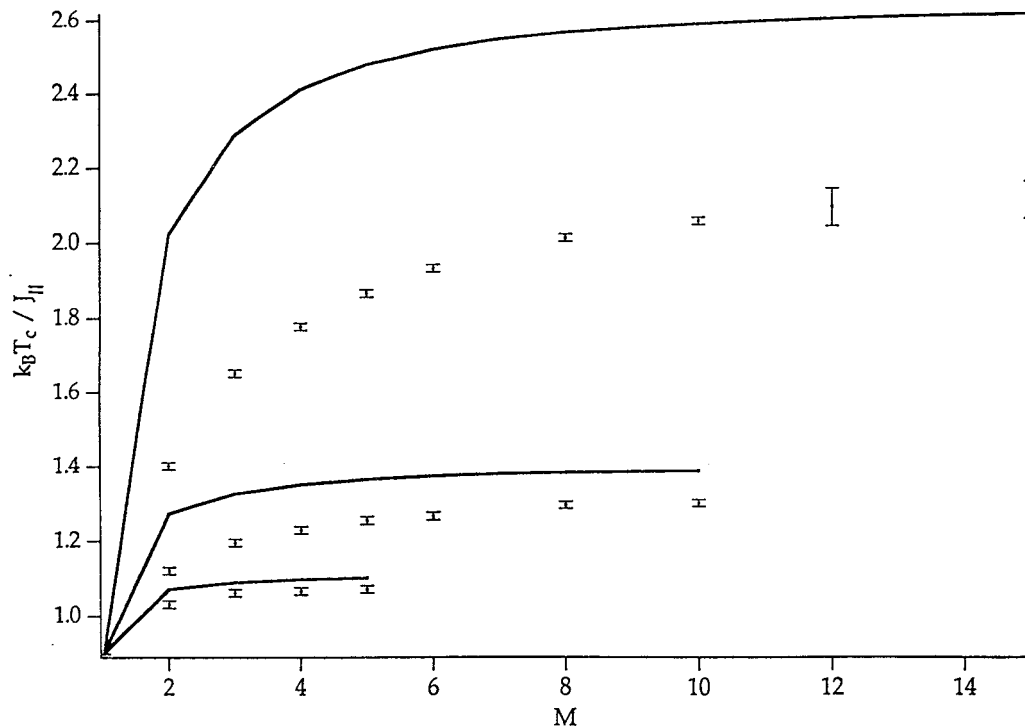


Figure 7: Critical temperature as a function of the number of planes for various anisotropies $J_{\perp}/J_{\parallel} = 1, 10^{-1}, 10^{-2}$ (top to bottom). The bars indicate the estimated error of the simulations. Full lines represent the mean-field results (with respect to J_{\perp} .)

cal) charges according to the renormalized harmonic approximation for spin waves yields a value of the critical temperature in excellent agreement with Monte Carlo calculations or high temperature expansions. Using the same approximation we obtained very satisfactory values for the exponents $\eta(T), \delta(T)$ along the critical line $0 < T < T_{KT}$ of the 2d XY model. One can conclude that, while the origin of the phase transition is presumably the unbinding of vortex-antivortex pairs, the critical behavior below this transition is essentially described by (anharmonic) spin waves.

Most part of this study was concerned with the 3d XY model in the limit of weak couplings in one and strong couplings in the other two directions. We have used various methods for determining the critical temperature both for the infinite system and for a finite number of weakly coupled planes, in particular a mean-field approach with respect to the weak coupling, scaling arguments and Monte Carlo simulations. The comparison between the different methods has shown that for very weak coupling in z -direction vortex loops parallel to the $a-y$ planes play a dominant role. At the same time the energetics of these excitations and their coupling to the elastic degrees of freedom remains to be clarified.

The extreme sensitivity of a system of uncoupled planes with respect to any interplane coupling, as small as it may be, has been demonstrated by means of the

spontaneous magnetization, which is rigorously zero at finite temperatures in the 2d case, but of order one below the critical temperature for interplane couplings that are many orders of magnitude smaller than the intraplane coupling.

We finally discuss the connection to real materials. The most obvious examples are quasi-two-dimensional Heisenberg ferromagnets with a large anisotropy term forcing the spins to remain essentially planar. Several examples have been studied experimentally; an extensive review has been given by de Jongh and Miedema³¹. An interesting connection between the 2d magnetization in a magnetic field, Eq. (5.5), and experiments on a layered magnet with weak antiferromagnetic couplings between planes has been made by Patashinskii and Pokrovskii¹¹. At a certain critical magnetic field applied to this system the antiferromagnetic ordering between planes is destroyed and the system may be considered as a collection of independent planes in a field. The agreement between the renormalized harmonic approximation and the experimentally determined exponent is encouraging.

The connection with superfluid films or layered superconductors is more subtle³². In both cases a two-component field represents the complex order parameter of the superfluid phase. The mapping onto the XY model is achieved by freezing the amplitude of the field and allowing only phase fluctuations. With this

assumption one neglects large amplitude fluctuations associated with points (or lines) where the field vanishes³³. In a superconductor, which corresponds to a charged Bose fluid, one has also to take into account fluctuations of the electromagnetic field. These may change the nature of the phase transition^{34,35}. An interesting problem arises in this context for a system of planes coupled exclusively by the electromagnetic field. Neglecting both amplitude fluctuations and vortex loops perpendicular to the planes, one obtains a transition of the Kosterlitz-Thouless type, at least using the Coulomb gas analogy in its low temperature limit²¹.

We finally discuss the recent experiments on superlattices consisting of superconducting sheets separated by non-superconducting layers²⁴⁻²⁸. For large separation of the superconducting layers, these can be considered as independent systems of finite thickness. The observed dependence of the critical temperature on this thickness is in qualitative agreement with Figure 7, although much more pronounced. In fact, it is not clear to what extent two-dimensional fluctuations are responsible for the strong decrease in T_c with decreasing thickness, as other mechanisms can lead to qualitatively similar results³⁶⁻⁴¹.

Acknowledgments

One of us (A.C.) would like to thank Ph. de Forcrand for providing a copy of his Monte Carlo program. We have profitted from stimulating discussions with B. Horowitz, S.E. Korshunov, J.M. Kosterlitz, A.I. Larkin, and A. Vallat. This work has partly been supported by the Swiss National Foundation through the grant Nr. 21-29021.90.

Appendix A: Duality transformation

We generalize here the analysis devised by Savit⁶ for the isotropic 3d XY model to the anisotropic case. The partition function for the Hamiltonian (2.3) is

$$Z = \prod_{\mathbf{R}} \left[\int_{-\pi}^{\pi} \frac{d\vartheta(\mathbf{R})}{2\pi} \right] \exp \left\{ \beta \sum_{\mathbf{R}, \mu} J_{\mu} \cos [\vartheta(\mathbf{R} + \mathbf{e}_{\mu}) - \vartheta(\mathbf{R})] \right\}, \quad (\text{A.1})$$

where \mathbf{e}_{μ} is a unit vector in direction μ , $\mathbf{p} = x, y, z$, and the exchange constants are $J_x = J_y = J_{\parallel}$, $J_z = J_{\perp}$. We

first use the character expansion

$$\exp \{ \beta J_{\mu} \cos [\vartheta(\mathbf{R} + \mathbf{e}_{\mu}) - \vartheta(\mathbf{R})] \} = \sum_{n_{\mu}(\mathbf{R})=-\infty}^{\infty} I_{n_{\mu}(\mathbf{R})}(\beta J_{\mu}) \cdot \exp \{ i n_{\mu}(\mathbf{R}) [\vartheta(\mathbf{R} + \mathbf{e}_{\mu}) - \vartheta(\mathbf{R})] \}, \quad (\text{A.2})$$

where $I_n(x)$ is the modified Bessel function of order n . We naturally associate the integer $n_{\mu}(\mathbf{R})$ with the (directed) link from \mathbf{R} to $\mathbf{R} + \mathbf{e}_{\mu}$. Inserting Eq. (A.2) into Eq. (A.1) and regrouping terms (using periodic boundary conditions) we obtain

$$Z = \sum_{\{n_{\mu}(\mathbf{R})\}} \prod_{\mathbf{R}, \mu} [I_{n_{\mu}(\mathbf{R})}(\beta J_{\mu})] \prod_{\mathbf{R}} \left[\int_{-\pi}^{\pi} \frac{d\vartheta(\mathbf{R})}{2\pi} \right] \exp \left\{ -i \sum_{\mathbf{R}, \mu} \vartheta(\mathbf{R}) \Delta_{\mu} n_{\mu}(\mathbf{R}) \right\}, \quad (\text{A.3})$$

where

$$\Delta_{\mu} n_{\mu}(\mathbf{R}) = n_{\mu}(\mathbf{R}) - n_{\mu}(\mathbf{R} - \mathbf{e}_{\mu}) \quad (\text{A.4})$$

is the (non-symmetrized) lattice derivative. The angular integration is now easily performed; it yields the constraint

$$\sum_{\mu} \Delta_{\mu} n_{\mu}(\mathbf{R}) = 0, \quad \forall \mathbf{R}. \quad (\text{A.5})$$

The condition (A.5) allows us to use the parametrization

$$n_{\mu}(\mathbf{R}) = \sum_{\lambda, \nu} \epsilon_{\mu\nu\lambda} \Delta_{\nu} A_{\lambda}(\mathbf{R} - \mathbf{e}_{\lambda}), \quad (\text{A.6})$$

where the variables $A_{\lambda}(\mathbf{R})$ are integers naturally associated with the links of the dual lattice (with vectors \mathbf{R} at the midpoints of the unit cells of the original lattice). The relation (A.6) is illustrated in Figure 8. The partition function can now be written as

$$Z = \sum_{\{n_{\mu}(\mathbf{R})\}} \exp \left\{ \sum_{\mathbf{R}, \mu} \log I_{n_{\mu}(\mathbf{R})}(\beta J_{\mu}) \right\} \sim \sum_{\{n_{\mu}(\mathbf{R})\}} \exp \left\{ \sum_{\mathbf{R}, \mu} \sum_{p=1}^{\infty} \frac{1}{p!} D_p(\beta J_{\mu}) n_{\mu}^{2p}(\mathbf{R}) \right\}, \quad (\text{A.7})$$

where the $D_p(\beta J_{\mu})$ are cumulants of the functions

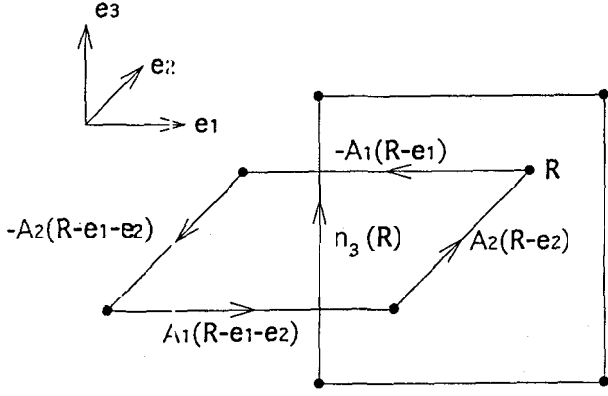


Figure 8: Original lattice link variable n , and associated plaquette of the dual lattice.

$$T_p(\beta J_\mu) = \frac{(-1)^p}{(2p)!} \frac{p!}{\pi I_0(\beta J_\mu)} \int_0^\pi d\omega \omega^{2p} e^{\beta J_\mu \cos \omega}, \quad (\text{A.8})$$

i.e. $D_1 = T_1$, $D_2 = T_2 - T_1^2$, $D_3 = T_3 - 2T_1T_2 - 2T_1^3$, etc.. In Eq. (A.7) we have dropped a constant $\prod_\mu [I_0(\beta J_\mu)]^N$

We consider now the low temperature limit $\beta J_\mu \gg 1$, $\mu = x, y, z$. In this limit the leading contribution to D_p is proportional to $(\beta J_\mu)^{1-2p}$ [6] and therefore we retain only the term D_1 given by

$$D_1(\beta J_\mu) \sim -\frac{1}{2\beta J_\mu}. \quad (\text{A.9})$$

The partition function (A.7) now reads

$$Z = \sum'_{\{A_\mu(\mathbf{R})\}} \exp \left\{ -\sum_{\mathbf{R}, \mu} \frac{1}{2\beta J_\mu} \left[\sum_{\nu, \lambda} \epsilon_{\mu\nu\lambda} \Delta_\nu A_\lambda(\mathbf{R} - \mathbf{e}_\lambda) \right]^2 \right\}, \quad (\text{A.10})$$

where we have inserted Eq. (A.6). The prime indicates that, in order to avoid overcounting configurations $\{n_\mu(\mathbf{R})\}$, a particular gauge has to be chosen for the variables $\mathbf{A}, (\mathbf{R})$. We choose the gauge

$$\mathbf{A}, (\mathbf{R}) = 0 \quad \forall \mathbf{R}. \quad (\text{A.11})$$

Using the Poisson summation formula⁴² we can replace the discrete variables $A_\mu(\mathbf{R})$ by new discrete variables $\ell_\mu(\mathbf{R})$ and continuum variables $\Phi_\mu(\mathbf{R})$ giving

$$Z = \sum'_{\{\ell_\mu(\mathbf{R})\}} \prod_{\mathbf{R}, \mu} \left[\int_{-\infty}^{\infty} d\Phi_\mu(\mathbf{R}) \right] \cdot \exp \left\{ -\sum_{\mathbf{R}, \mu} \left[\frac{1}{2\beta J_\mu} \left(\sum_{\nu, \lambda} \epsilon_{\mu\nu\lambda} \Delta_\nu \Phi_\lambda(\mathbf{R} - \mathbf{e}_\lambda) \right)^2 \right] \right\}$$

$$\cdot \exp \left\{ \sum_{\mathbf{R}, \mu} [2\pi i \ell_\mu(\mathbf{R}) \Phi_\mu(\mathbf{R})] \right\}, \quad (\text{A.12})$$

where the sum is over configurations given in terms of $\ell_x(\mathbf{R}), \ell_y(\mathbf{R})$ only. Thus there are two independent variables $\ell_\mu(\mathbf{R})$ at each site \mathbf{R} of the dual lattice. As shown by Savit⁶ this gauge-dependent ensemble of configurations can be replaced by a gauge-independent ensemble $\{\ell_\mu(\mathbf{R})\}, \mu = x, y, z$ together with the constraint

$$\sum_\mu \Delta_\mu \ell_\mu(\mathbf{R}) = 0 \quad , \quad \forall \mathbf{R}. \quad (\text{A.13})$$

The variables $\ell_\mu(\mathbf{R})$ are interpreted as integer-valued "currents" flowing from \mathbf{R} to $\mathbf{R} + \mathbf{e}_\mu$. Eq. (A.13) implies that these currents form closed loops in the dual lattice. Performing the Gaussian integrations in Eq. (A.12) we obtain the final form of the partition function

$$Z = Z_s \cdot \sum_{\{\ell_\mu(\mathbf{R})\}} \exp \left\{ -2\pi^2 \beta \sum_{\mathbf{R}, \mathbf{R}', \mu} \ell_\mu(\mathbf{R}) V_\mu(\mathbf{R} - \mathbf{R}') \ell_\mu(\mathbf{R}') \right\}, \quad (\text{A.14})$$

where Z_s is the partition function in the spin wave approximation (i.e. with respect to \mathbf{H} , defined in Eq. (2.6)) and $V_\mu(\mathbf{R} - \mathbf{R}')$ is given by Eq. (2.20).

Appendix B: Mean-field approximation for the interplane coupling

We want to replace the coupling between planes by an effective field h_0 . Thus we introduce the mean-field Hamiltonian

$$H_0 = -J_\parallel \sum_{\langle \mathbf{R}, \mathbf{R}' \rangle} \mathbf{S}(\mathbf{R}) \cdot \mathbf{S}(\mathbf{R}') - (h + h_0) \sum_{\mathbf{R}} S_x(\mathbf{R}), \quad (\text{B.1})$$

where the first sum runs over nearest neighbor pairs within the planes. We use the Bogoliubov inequality for the Gibbs potential and determine h_0 by minimizing the r.h.s. of Eq. (3.9). A straightforward calculation then yields

$$h_0 = 2J_\perp M(h + h_0) \quad (\text{B.2})$$

where

$$M = \langle S_x(\mathbf{R}) \rangle_0 \quad (\text{B.3})$$

is the magnetization with respect to the Hamiltonian H_0 . The susceptibility above the critical temperature is found to be

$$\chi = \frac{\partial M}{\partial h} = \beta \left(1 + \frac{\partial h_0}{\partial h} \right) \frac{1}{N} \sum_{\mathbf{R}, \mathbf{R}'} \langle S_x(\mathbf{R}) S_x(\mathbf{R}') \rangle_0. \quad (\text{B.4})$$

The Hamiltonian (B.1) corresponds to uncoupled planes in an effective magnetic field $h+h_0$. Furthermore $h_0 = 0$ for $T > T_c$, so that in the limit $h \rightarrow 0$

$$\frac{\beta}{N} \sum_{\mathbf{R}, \mathbf{R}'} \langle S_x(\mathbf{R}) S_x(\mathbf{R}') \rangle_0 = \chi_{2d} \quad (\text{B.5})$$

is the susceptibility of the two-dimensional XY model. Combining Eqs. (B.2), (B.4), (B.5) we obtain

$$\chi = \frac{\chi_{2d}}{1 - 2J_{\perp} \chi_{2d}}. \quad (\text{B.6})$$

This procedure is readily generalized for the case of a finite number M of planes with open boundary conditions. We introduce inhomogeneous mean fields $h_{0\ell}, \ell = 1, \dots, M$, and corresponding susceptibilities

$$\chi_{\ell} = \frac{\partial M_{\ell}}{\partial h}. \quad (\text{B.7})$$

where M_{ℓ} is the magnetization of the ℓ -th plane. This yields a system of linear equations

$$\chi_{\ell} = (1 + J_{\perp} \chi_{\ell-1} + J_{\perp} \chi_{\ell+1}) \chi_{2d}, \quad \ell = 1, \dots, M \quad (\text{B.8})$$

($\chi_{M+1} = \chi_0 = 0$). These are easily diagonalized. The critical temperature for the case of M planes is determined by the vanishing of the lowest eigenvalue of the associated homogeneous system, giving

$$1 = 2J_{\perp} \cos\left(\frac{\pi}{M+1}\right) \chi_{2d}(T_c). \quad (\text{B.9})$$

Appendix C: Ginzburg-Landau theory

An equivalent field formulation of the XY model, which leads to the Ginzburg-Landau theory in the vicinity of the mean-field transition temperature, has been derived by Kleinert⁴³. The partition function (Eq. (A.1) of Appendix A) can be rewritten as

$$Z = \prod_{\mathbf{R}} \left[\int_{-\pi}^{\pi} \frac{d\vartheta(\mathbf{R})}{2\pi} \right] \exp \left\{ \beta J_0 \sum_{\mathbf{R}, \alpha} S_{\alpha}(\mathbf{R}) D S_{\alpha}(\mathbf{R}) \right\}, \quad (\text{C.1})$$

where $J_0 = 2J_{\parallel} + J_{\perp}$, $S_{\alpha}(\mathbf{R}), \alpha = 1, 2$, are the x - and y -components of the unit vector

$$\mathbf{S}(\mathbf{R}) = (\cos \vartheta(\mathbf{R}), \sin \vartheta(\mathbf{R})). \quad (\text{C.2})$$

The operator D reads

$$D = 1 + \frac{1}{2J_0} \left[J_{\parallel} (\tilde{\Delta}_x \Delta_x + \tilde{\Delta}_y \Delta_y) + J_{\perp} \tilde{\Delta}_z \Delta_z \right], \quad (\text{C.3})$$

where Δ , and $\tilde{\Delta}_{\mu}$ are lattice derivatives

$$\begin{aligned} \Delta_{\mu} f(\mathbf{R}) &= f(\mathbf{R}) - f(\mathbf{R} - \mathbf{e}_{\mu}), \\ \tilde{\Delta}_{\mu} f(\mathbf{R}) &= f(\mathbf{R} + \mathbf{e}_{\mu}) - f(\mathbf{R}). \end{aligned} \quad (\text{C.4})$$

The spin variables in Eq. (C.1) can be formally decoupled by introducing the two-component field $\mathcal{S} = (\psi_1, \psi_2)$. Indeed, one verifies that Eq. (C.1) is equivalent to the expression

$$Z = \prod_{\mathbf{R}} \left[\frac{1}{4\pi\beta J_0} \int_{-\infty}^{\infty} d\psi_1(\mathbf{R}) \int_{-\infty}^{\infty} d\psi_2(\mathbf{R}) \int_{-\pi}^{\pi} \frac{d\vartheta(\mathbf{R})}{2\pi} \right] \exp \left\{ - \sum_{\mathbf{R}, \alpha} \left[\frac{1}{4\beta J_0} \psi_{\alpha}^2(\mathbf{R}) + S_{\alpha}(\mathbf{R}) (D^{1/2} \psi_{\alpha})(\mathbf{R}) \right] \right\} \quad (\text{C.5})$$

The angular integration is easily carried out and we find

$$Z = \prod_{\mathbf{R}, \alpha} \left[\int_{-\infty}^{\infty} \frac{d\psi_{\alpha}(\mathbf{R})}{\sqrt{4\pi\beta J_0}} \right] \exp(-\beta F \{ \psi_{\alpha}(\mathbf{R}) \}), \quad (\text{C.6})$$

where the free energy functional is given by

$$\beta F = \sum_{\mathbf{R}} \left[\frac{|\psi(\mathbf{R})|^2}{4\beta J_0} - \log I_0 \left\{ |(D^{1/2} \psi)(\mathbf{R})| \right\} \right]. \quad (\text{C.7})$$

Expanding $\log I_0$ up to fourth order in ψ and up to second order in $\Delta_{\mu} \psi$ we finally obtain

$$\begin{aligned} \beta F &= \sum_{\mathbf{R}} \left\{ \frac{1}{8J_0} \sum_{\mu} [J_{\parallel} (\Delta_{\mu} \psi_{\alpha}(\mathbf{R}))^2 \right. \\ &+ J_{\parallel} (\Delta_y \psi_{\alpha}(\mathbf{R}))^2 + J_{\perp} (\Delta_z \psi_{\alpha}(\mathbf{R}))^2] \\ &+ \frac{1}{4} \left(\frac{1}{\beta J_0} - 1 \right) |\psi(\mathbf{R})|^2 + \frac{1}{64} |\psi(\mathbf{R})|^4 \left. \right\}. \end{aligned} \quad (\text{C.8})$$

Appendix D: Monte Carlo procedure

Until rather recently, the study of the critical region using Monte Carlo techniques seemed impossible because of two reasons. First, in a simulation one is restricted to models with a finite number of sites, while being interested in the thermodynamic limit. This finiteness introduces among other effects shifts in the critical temperatures and a smoothing of the transition peaks. To minimize these finite-size effects, the size of the simulated model should be much larger than the correlation length of the system, which is going to diverge near a critical point. So one has to simulate very large systems, and this is difficult, because the computational effort necessary to achieve a given accuracy

scales like L^d , where L is the number of sites along one direction and d is the dimension of space. Second, in a Monte Carlo simulation, physical quantities are estimated by sampling over a set of configurations generated by a type of random walk, each new configuration being obtained from the preceding one through simple rules. Successive configurations are then correlated, and the amount of correlation depends on the probabilities of transition between configurations, which themselves depend on the temperature at which the simulation is performed. Accordingly, the size of the sample needed to achieve a given accuracy, and therefore the number of configurations to generate, is going to depend on temperature.

It occurs that for a large class of Monte Carlo algorithms (like spin-flip Metropolis algorithm or heat-bath algorithm), this number of configurations scales like $(\min(L, \xi))^z$, where ξ is the correlation length of the (infinite) model and z is called *dynamical critical exponent*, with typical value ≈ 2 . If the correlation length is small this factor will be negligible, but near a critical transition it will be very important. This phenomenon is called "critical slowing down". Therefore, in the critical region, one is faced with two simultaneous problems with these algorithms :

1. Very large systems must be studied to avoid finite-size effects.
2. The number of configurations one has to generate increases.

In practice, this prevents precise studies of the critical region: large systems require a great deal of computer effort to generate new configurations, and even more configurations are needed as one approaches the critical point. The solution to this problem has come from the introduction of new types of algorithms, called *cluster updating* algorithms^{44,45}, which are characterized by smaller values of z ($z \leq 0.2$), and hence reduced critical slowing down. This has allowed studies of the critical region.

Here, we have studied models of size $L \times L \times M$, with L between 16 and 64, and M , the number of layers, between 2 and 15. We want to calculate the critical temperature T_c in the $L \rightarrow \infty$ limit as a function of M , the number of layers and the anisotropy J_{\perp}/J_{\parallel} . Periodic boundary conditions are assumed in the x and y directions, while free boundary conditions are taken in the z direction. We have used Wolff's cluster algorithm⁴⁵ to generate the configurations. For all system sizes up to $M=10$, each spin has been updated (on the average) at least 5000 times for the sampling, and 500 times for relaxation. Runs with larger values of L and larger number of sweeps have also been performed to check the stability of the results. The localization of the critical point has been achieved by using Binder's fourth order cumulant for the magnetization⁴⁶

which should take a unique value at T_c , independent of L up to finite-size effects of order $\mathcal{O}(1/L)$. Finite-size scaling to the $L \rightarrow \infty$ limit has been used.

References

1. N. D. Mermin and H. Wagner, Phys. Rev. Lett. 22, 1133 (1966).
2. P. C. Hohenberg, Phys. Rev. 158, 383 (1967).
3. V. L. Berezinskii, Sov. Phys. JETP 32, 493 (1970); 34, 610 (1971).
4. J. M. Kosterlitz and D.J. Thouless, J. Phys. C 6, 1181 (1973).
5. C. Itzykson and J.-M. Drouffe, Statistical Field Theory, (Cambridge University Press, 1989).
6. R. Savit, Phys. Rev. B 17, 1340 (1978).
7. P. R. Thomas and M. Stone, Nucl. Phys. B 144, 513 (1978).
8. J. Villain, J. Physique 36, 581 (1975).
9. J. V. José, L.P. Kadanoff, S. Kirkpatrick and D.R. Nelson, Phys. Rev. B 16, 1217 (1977).
10. E. Eisenriegler, Phys. Rev. B 9, 1029 (1974).
11. A. Z. Patashinskii and V.I. Pokrovskii, Fluctuation Theory of Phase Transitions, (Pergamon Press, Oxford, 1979).
12. J. M. Kosterlitz, J. Phys. C7, 1046 (1974).
13. P. Butera, M. Comi, and G. Marchesini, Phys. Rev. B40, 534 (1989) and private communication.
14. C. R. Allton and C. J. Hamer, J. Phys. A21, 2417 (1988).
15. Th. Niemeijer and J. M. J. van Leeuwen, Phys. Rev. Lett. 31, 1411 (1973).
16. S. Hikami and T. Tsuneto, Prog. Theor. Phys. 63, 387 (1980).
17. J. Epiney and Ph. de Forcrand, unpublished.
18. G. Kohring, R. E. Shrock, and P. Wills, Phys. Rev. Lett. 57, 1358 (1986).
19. J. Friedel, J. Physique 49, 1561 (1988).
20. J. Friedel, J. Phys.: Condens. Matter 1, 7757 (1989).
21. S. E. Korshunov, Europhys. Lett. 11, 757 (1990).
22. W. Janke and T. Matsui, Phys. Rev. B 42, 10673 (1990).
23. D. J. Bishop and J. D. Reppy, Phys. Rev. B22, 5171 (1980).
24. J.-M. Triscone, O. Fischer, O. Brunner, L. Antognazza, A. D. Kent and M. G. Karkut, Phys. Rev. Lett. 64, 804 (1990).
25. Q. Li, X. X. Xi, X. D. Wu, A. Inam, S. Vadlamantati, W. L. McLean, T. Venkatesan, R. Ramesch, D. M. Hwang, J. A. Martinez and L. Nazar, Phys. Rev. Lett. 64, 3086 (1990).
26. A. Gupta, R. Gross, E. Ollsson, A. Segmuller, G. Koren and C.C. Tsuei, Phys. Rev. Lett. 64, 3191 (1990).

27. D. H. Lowndes, D. P. Norton and J. D. Budai, *Phys. Rev. Lett.* 65, 1160 (1990).
28. G. Jakob, P. Przyslupski, C. Stolzel, C. Tomé-Rosa, A. Walkenhorst, M. Schmitt, and H. Adrian, *Physica C* 185-189, 2087 (1991).
29. M. Zamora, A. Chiolero, X. Bagnoud, and D. Baeriswyl, *Helv. Phys. Acta* 65, 456 (1992).
30. A. Schmidt and T. Schneider, *Helv. Phys. Acta* 65, 484 (1992); *Z. Phys. B* 87, 265 (1992).
31. L. J. de Jongh and A. R. Miedema, *Adv. Phys.* 23, 1 (1974).
32. For a recent review see P. Minnhagen, *Rev. Mod. Phys.* 59, 1001 (1987).
33. For a discussion of this point see B. I. Halperin, in *Physics of Low-Dimensional Systems*, ed. by Y. Nagaoka and S. Hikami, (Publication Office, Prog. Theor. Phys., 1979).
34. B. I. Halperin, T. C. Lubensky, and S.-K. Ma, *Phys. Rev. Lett.* 32, 292 (1974).
35. S. Kolnberger and R. Folk, *Phys. Rev. B* 41, 4083 (1990).
36. D. Ariosa and H. Beck, *Phys. Rev. B* 43, 344 (1991).
37. T. Schneider, *Z. Phys. B* 85, 187 (1991).
38. J. Z. Wu, C. S. Ting, W. K. Chu, and X. X. Yao, *Phys. Rev. B* 44, 411 (1991).
39. M. Rasolt, T. Edis, and Z. Tešanovic, *Phys. Rev. Lett.* 66, 2927 (1991).
40. D. Baeriswyl and X. Bagnoud, unpublished.
41. R. Fehrenbacher and T. M. Rice, preprint.
42. R. Courant and D. Hilbert, *Methods of Mathematical Physics* (Wiley, New York, 1966).
43. H. Kleinert, *Gauge Fields in Condensed Matter*, (World Scientific, Singapore, 1989).
44. R. H. Swendsen and J. S. Wang, *Phys. Rev. Lett.* 58, 86 (1987).
45. U. Wolff, *Phys. Rev. Lett.* 62, 361 (1989).
46. K. Binder, *Phys. Rev. Lett.* 47, 693 (1981).